

Suppression of High Transverse Momentum π^0 Spectra in Au+Au Collisions at RHIC.

D. E. Kahana

31 Pembroke Dr., Stony Brook, NY 11790, USA

S. H. Kahana

Physics Department, Brookhaven National Laboratory
Upton, NY 11973, USA

(Dated: February 5, 2008)

Au+Au, $s^{1/2} = 200$ A GeV measurements at RHIC, obtained with the PHENIX, STAR, PHOBOS and BRAHMS detectors, have all indicated a suppression of production, relative to an appropriately normalized NN level. For central collisions and vanishing pseudo-rapidity these experiments exhibit suppression in charged meson production, especially at medium to large transverse momenta. In the PHENIX experiment similar behavior has been reported for π^0 spectra.

In a recent work [1] on the simpler D+Au interaction, to be considered perhaps as a tune-up for Au+Au, we reported on a pre-hadronic cascade mechanism which can explain the mixed observation of moderately reduced p_{\perp} suppression at higher pseudo-rapidity as well as the Cronin enhancement at mid-rapidity. Here we present the extension of this work to the more massive ion-ion collisions.

Our major thesis is that much of the suppression is generated in a late stage cascade of colourless pre-hadrons produced after an initial short-lived coloured phase. We present a pQCD argument to justify this approach and to estimate the time duration τ_p of this initial phase. Of essential importance is the brevity in time of the coloured phase existence relative to that of the strongly interacting pre-hadron phase, the latter essentially an interactive cascade. These distinctions in phase are of course not strict, but adequate for treating the suppression of moderate and high p_{\perp} mesons.

PACS numbers: 25.75.-q, 12.38.Mh, 24.10.Jv

I. INTRODUCTION

The specific question we deal with in this work is the suppression of medium to high transverse momentum meson yields observed in the experimental measurements [2, 3, 4, 5] for Au+Au at 130 GeV and 200 GeV. The experiments have focused on the η and p_{\perp} -dependence of the ratio of these yields to those in p+p, for charged particles:

$$R[AA/NN] = \left(\frac{1}{N_{coll}} \right) \frac{[d^2 N^{ch}/dp_{\perp} d\eta] (AA)}{[d^2 N^{ch}/dp_{\perp} d\eta] (NN)}, \quad (1)$$

where N_{coll} is a calculated number of binary NN collisions occurring in Au+Au at a designated energy and centrality. One can also, of course, just compare the yields directly to the data without reference to ratios.

The simulation code LUCIFER, developed for high energy heavy-ion collisions, has previously been applied to both SPS energies $s^{1/2} = (17.2, 20)$ A GeV [6, 7, 8] and to RHIC energies $s^{1/2} = (56, 130, 200)$ A GeV [6, 8]. Although nominally intended for dealing with soft, low p_{\perp} interactions, it is possible to introduce high p_{\perp} hadron spectra via the NN inputs, which form the building blocks of the simulations, and thus to examine the effect of re-scattering, and concomitant energy loss, on the high p_{\perp} spectra [1]. The simulation is divided into two phases I and II. The first stage sets up the participants, both mesonic and baryonic, their four momenta and positions for the commencement of a ‘hadronic’ cascade in phase II. Energy loss and interactions within what amounts to a ‘hadronic’ fluid in phase II play a key role in the eventual suppression of the transverse momentum distributions.

This approach has already yielded a consistent description of at least the final stage phenomena leading to measurements in both $D + Au$ [1] and $Au + Au$ at a variety of kinematical conditions, energies and transverse momenta. All these results follow given only the presence at early times during the ion-ion collision of a fluid of ‘pre-hadrons’ having rather generic properties.

Such a mechanism for the suppression of high transverse momentum jets may seem to run counter to the conventional pQCD view. There does exist, however, notable justification for a picture in which colourless pre-hadrons, may be produced at rather early times in a AA collision, and then play a key role in the further development of the system. First there is the work of Shuryak and Zahed [9] on the persistence of hadron-like states above the critical temperature in a dense quark-gluon medium as well as similar results from lattice-driven studies on the persistence of the J/Ψ and other special hadronic states [10]. Recently a much more direct treatment has been given, on which we now mainly rely, by Kopeliovich, Nemchik and Schmidt [11] as well as Berger [12], who directly consider the temporal dynamics

of pre-hadron production from a pQCD point of view. In particular Kopeliovich *et al.*, outline the fate of leading hadrons from jets, in deep inelastic scattering (DIS) on massive ions and discuss the relevance to relativistic heavy ion collisions. These works have the distinct advantage of relying directly on pQCD. We attempt to reproduce their development, as it is germane to our treatment of NN, NA and AA interactions.

Figure (1), essentially borrowed from Reference(11), displays the production of a jet, here at least a moderately high energy quark, in a pp or pA event and the time scales relevant to the process. Kopeliovich *et al.* begin by explicitly considering eP or eA, in which case the initiating particle in the jet creation is an off-shell photon (γ^*). In pp or AA one could equally well employ a gluon at the first vertex. The kinematics [11] remains essentially the same then for nuclear induced events and we elaborate this case somewhat.

The essential feature evident in the figure is the production of a colour neutral pre-hadron after a time t_p , from an initially perturbative high p_\perp quark, by what one could label as coalescence of the leading quark with an ambient anti-quark. This coalescence incidentally is most probable for co-moving anti-quarks, the scarcity of co-movers with increasing p_\perp explaining the rapid fall off of even the pp meson spectrum with increasing p_\perp . Also prominent in this diagram are the early perturbative gluon radiation. These radiated gluons may in due course create further pre-hadrons, and of course there is then a concomitant energy loss from the initial quark. Further, for leading partons, one expects that the hadronisation time t_h is considerably longer than t_p , involving soft processes that eventually put the pre-hadron on its final hadronic mass shell. Octet $q\bar{q}$'s might also arise but will not persist or eventually coalesce given the repulsive or non-confining forces in such systems.

One can summarise the kinematic arguments [11] most easily in the rest frame of the struck proton or nucleus. We use these arguments to estimate the production time t_p for the pre-hadron, which will be a considerably shorter time τ_p in the colliding frame of an AA system. For DIS on a nucleon, on its own or within a nucleus A, the production time in Figure (1) is estimated to be

$$t_p \sim \frac{[E_q]}{[dE_q/dz]}(1 - z_h), \quad (2)$$

where z_h is the fraction of quark energy imparted to the hadron. Integrating the gluon radiation spectrum one obtains for the energy loss per unit length z , a time independent rate [11, 13] rising quadratically with the hard scale Q ,

$$-\frac{DE}{Dz} = \frac{2\alpha_s}{3\pi}Q^2. \quad (3)$$

The colour neutralisation time is then given by:

$$t_p \sim \frac{E_q}{Q^2}(1 - z_h). \quad (4)$$

The hadronisation time is related to the QCD scale factor and is usually estimated as:

$$t_h \sim \frac{E_h}{\Lambda_{QCD}^2}(1 - z_h), \quad (5)$$

and is much longer than the colour neutralisation time, given that the QCD scale is close to 200 GeV.

The authors of Reference (11) argue the brevity of the de-colourisation time scale is a consequence of energy conservation, coherence and Sudakov suppression.

Importantly, a much reduced scale for pre-hadron creation is likely to remain true even for non-leading partons provided Equation (4) remains valid, *i. e.* when Q is comparable to E_q . Thus many of the radiated hard or even moderately hard gluons, in the early stages of a pp or AA collision will initiate similar pre-hadrons, and in a nuclear medium such large sized objects will be sufficiently numerous and of critical importance to the dynamics. One should keep in mind that the overall multiplicity is not large at $p_\perp \geq 1$ GeV/c, where the NN spectra (see Figure (5)) has dropped from that at the softest transverse momenta measured by close to two orders of magnitude and for Au+Au (Figure 7) by somewhat more.

One concludes that the production and hadronisation processes are to some degree separate: with generally t_p less than t_f and frequently much less. Corresponding time scales in, say, the center of momentum frame for an A+A system will of course be considerably contracted. Although the colourless pre-hadron in Figure (1) is generated by an initially perturbative process with an anti-quark, it is the subsequent interactions with other such pre-hadrons that leads to the observed suppression for mesons of appreciable and even moderate transverse momentum. The pre-hadron

perturbatively begins life with the $q\bar{q}$ at small relative distance, and thus has a small initial size, but in light of the ambient momenta for such high or even moderately high energy partons, the transverse diameter rapidly increases to the scale of a typical hadron. Reference (11) suggests the entire growth to pre-hadronic size occurs quickly.

One can pursue the evolution of the system of pre-hadrons via a Glauber-theory [11, 14] based treatment of their interactions, or, as we do, via a standard cascade model. The end result is little different: what has been labelled jet suppression results. In Glauber theory the hadron-sized cross-sections produce strong absorption: and hard pre-hadrons simply do not remain in the final state, they are too often absorbed. In the cascade described hereafter the pre-hadronic medium is sharply cooled by the interactions and instead of on hard meson, many soft mesons appear, and at lower p_\perp .

To obtain the final cascade yields for both D+Au [1] and Au+Au, it is essential that the characteristic time t_p be considerably less than t_f . Indeed this constraint plus the appropriately large pre-hadron interaction cross-sections are also instrumental in generating the surprisingly large elliptical flow that has been measured at RHIC [15, 16]. References (11,12) provide a perturbative QCD justification for both such conditions, the early de-colourisation and the large pre-hadron cross-sections.

For completeness we present a brief overview of the dynamics of our Monte Carlo simulation, which has already been described extensively in earlier works [1, 7]. Many other simulations of heavy ion collisions exist and these are frequently hybrid in nature, using say string models in the initial state [17, 18, 19, 20, 21, 22, 23, 24] together with final state hadronic collisions, while some are either purely or partly partonic [25, 26, 27, 28, 29, 30] in nature. Our approach is closest in spirit to that of RQMD and K. Gallmeister, C. Greiner, and Z. Xu [31] as well as work by W. Cassing [17, 31, 32] and G. Wolschin [33]. Certainly our results seem to parallel those of the latter authors. They seek to separate initial perhaps parton dominated processes from hadronic interactions occurring at some intermediate but not necessarily late time, or to rely on some hadronic dynamics.

The ostensible purpose of describing such high energy collisions without explicitly introducing the parton substructure of hadrons, at least for soft processes, was to set a baseline for judging whether deviations existed between simulation and experiment, which could then signal interesting phenomena. The division between soft and hard processes is not necessarily easy to identify in heavy ion data, although many authors believe they have accomplished this within a gluon-saturation picture [34, 35, 36]. For both D+Au and Au+Au systems we separate the effects of a second stage cascade, a lower energy but still early hadronic cascade, from those of the first stage, a parallel rather than sequential treatment of initial (target)-(projectile) NN interactions. The first, quite likely partonic, stage ends after some average time t_p . Paradoxically for us then, it is perhaps higher p_\perp meson production that is most justified by pQCD.

In the present work we do indeed find considerable suppression of the Au+Au transverse momentum spectrum at central rapidity. The key dynamics occur presumably after the de-colourisation phase in Reference (11), i. e. after some time closely related to the much contracted production time in the collision center of momentum frame $\tau_p \sim \gamma_{cm}^{-1} t_p$.

The first stage of our simulation, involving the collective interaction of the initially present nucleons, produces a ‘hot’ gas or liquid of pre-hadrons which is considerably cooled in an inevitably expanding and interacting final state cascade. This cooling produces the observed ‘jet’ suppression, and not surprisingly, that suppression is appreciably greater for Au+Au than for D+Au [1, 2]. It is clear that the early pre-hadron ‘medium’ resembles a rather dense fluid.

II. THE SIMULATION

A. Phase I

Phase I of LUCIFER considers the initial interactions between the separate nucleons in the colliding ions A+B, but is not a cascade. It amounts to a creation of the initial conditions for the final lower energy cascade. The totality of events in phase I involving each projectile particle happen essentially simultaneously or one might say in parallel. Energy loss due to pre-hadron production as well as the creation of transverse momentum (p_\perp), initial conditions for what follows, are occur in phase I. A model of NN collisions [6, 7], incorporating most known inclusive cross-section and multiplicity data, guides phase I. The two body model, clearly an input to our simulation, is fitted to the elastic, single-diffractive (SD) and non-single-diffractive (NSD) aspects [37] of high energy pp collisions [42, 43] and $P\bar{P}$ data [44]. The soft QCD aspects of early A+B events are then modeled through their incorporation in the phenomenological nucleon-nucleon inputs.

One notes it is precisely the energy dependence of the cross-sections and multiplicities of the NN input that led to our successful *prediction* [7] of the rather small ($\sim 13\%$) increase in $dN^{ch}/d\eta$ that was first observed between $s^{1/2} = 130$ and $s^{1/2} 200$ A GeV in the PHOBOS data [45].

A history of the collisions that occur between nucleons as they move along straight lines in phase I is recorded and later used to guide the determination of multiplicity. Collision driven random walk fixes the p_{\perp} to be ascribed to the baryons at the start of phase II. The overall multiplicity, however, is subject to a modification, based as we believe on natural physical requirements [6].

The collective/parallel method of treating many NN collisions between the target and projectile is achieved by defining a group structure for interacting baryons, which preserves the geometry of the nucleus-nucleus collision. This is best illustrated by considering a prototypical proton-nucleus (pA) collision. A group is defined by spatial contiguity. A nucleon at some impact parameter $b(\bar{x}_{\perp})$ is imagined to collide with a corresponding ‘row’ of nucleons sufficiently close in the transverse direction to the straight line path of the proton, *i. e.* within a distance corresponding to the NN cross-section. In a nucleus-nucleus (AB) collision this procedure is generalized by making two passes: on the first pass one includes all nucleons from the target which come within the given transverse distance of some initial projectile nucleon, then on the second pass one includes for each target nucleon so chosen, all of those nucleons from the projectile approaching it within the same transverse distance. This totality of mutually colliding nucleons, at similar transverse displacements, constitute a group. The procedure partitions target and projectile nucleons into a set of disjoint interacting groups as well as a set of non-interacting spectators in a manner depending on the overall geometry of the AB collision. Clearly the largest groups in pA will, in this way, be formed for small impact parameters b ; while for the most peripheral collisions the groups will almost always consist of only one colliding pN pair. Similar conclusions hold in the case of AB collisions.

In phase II of the cascade we treat the re-scattering of the pre-hadrons produced in phase I. These pre-hadrons, both baryonic and mesonic in type, are not physical hadron resonances or stable particles such as appear in the particle data tables, which can only materialize after the hadronisation time t_h is passed. Importantly, pre-hadrons, are allowed to interact starting at earlier times, *viz.* τ_p is comparable in fact to the nominal target-projectile crossing time $T_{AB} \sim 2R_{AB}/\gamma$. In practice we vary the effective time delay for pre-hadron collisions in phase II, between 0.2 and 0.4 fm/c in the center of velocity frame.

The pre-hadrons, when mesonic, may consist of a spatially close, loosely correlated quark and anti-quark pair, and are given a mass spectrum between m_{π} and 1.2 GeV, with appropriately higher upper and lower mass ranges for pre-hadrons including strange or heavier quarks. The Monte-Carlo selection of masses is then governed by a Gaussian distribution,

$$P(m) = \exp(-(m - m_0)^2/w^2), \quad (6)$$

with m_0 a selected center for the pre-hadron mass distribution and $w = m_0/4$ the width. For non-strange mesonic pre-hadrons $m_0 \sim 800$ MeV, and for strange $m_0 \sim 950$ MeV. Small changes in m_0 and w have little effect since the code is constrained to fit hadron-hadron data using Equation (6).

Too high an upper limit for m_0 would destroy the soft nature expected for most pre-hadron interactions when they finally decay into ‘stable’ mesons. The mesonic pre-hadrons have isospin structure corresponding to ρ , ω , or K^* , while the baryons, in present calculation, are constrained to range across the octet and decuplet.

B. Elementary Hadron-Hadron Model

The underlying NN interaction structure involved in phase I has been introduced in a fashion dictated by standard proton-proton modeling [37]. The components of this modeling, elastic, single diffractive (SD) and non-single diffractive (NSD) were introduced above. Fits are obtained to the existing two-nucleon data over a broad range of energies $s^{1/2}$, using the above pre-hadrons as an intermediate stage. No re-scattering, only decay of these intermediate structures is permitted in the purely NN calculation. Cross-sections in pre-hadron collisions were assumed to be the same size as hadron cross-sections, *i.e.* the same as the meson-baryon or meson-meson cross-section, at the same center of mass energy. Where hadron-hadron cross-sections are inadequately known we employ straightforward quark counting to estimate the scale. Specifically, meson-meson interactions are scaled to 4/9 of the known NN cross-sections, thus no new parameters are invoked. Indeed, since known data then constrains the pre-hadronic interaction, this approach is a parameter-free input to the AA dynamics.

The explicit fit to these cross-sections is displayed in Figure (2). To achieve this representation we employed, for example, a parametrization of the data at high energies which actually works down to 5 GeV:

$$\sigma_{tot} = 35.43 - \frac{33.4}{s^{0.545}} + \frac{45.23}{s^{0.458}} + 0.308 (-3.364 + \ln(s))^2, \quad (7)$$

taken from V. Ezhela *et al.* [38].

We have also created an extended fit to the elastic data using higher energy CDF measurements at 546 GeV and 1800 GeV [39]:

$$\sigma_{el} = 7.0 - \frac{10.0}{s^{0.545}} + \frac{10.0}{s^{0.458}} + 0.09(-3.364 + \ln(s))^2. \quad (8)$$

The second important aspect of the NN interactions are the multiplicities of produced particles, which are again taken from measured and analyzed data. We employ KNO [40] scaling, with very little loss of accuracy for the transverse momenta of leading mesons, presumably from jets; *i. e.* the probability of achieving a given multiplicity at a certain energy is simply a function of the ratio of that multiplicity to the mean multiplicity. To illustrate the fits, Figures (3,4) show two energies, bracketing those relevant to RHIC physics. Equally good representations of intervening energy multiplicity data are of course obtained. As noted by many authors [41] the KNO scaling begins to break down for the tails of the highest energy distribution (see Fig.3), but in a fashion which again would have very little quantitative effect on our presentation.

C. High Transverse Momenta

A question that has yet to be addressed concerns the high p_{\perp} tails included in our fits to NN interactions and thus in our calculations. In fact it is certainly to such high p_{\perp} produced particles that the arguments of Reference (11) best apply. We simply include high p_{\perp} meson events through inclusion in the basic hadron-hadron interaction which is of course an input to, rather than a result of, our simulation. Thus in Figure(5) we display the NSD $(1/2\pi p_{\perp})(d^2 N^{charged}/dp_{\perp} d\eta)$ from UA1 [43].

One can use a single exponential together with a power-law tail in p_{\perp} , or alternatively two exponentials, to achieve a fit to UA1 $s^{1/2}=200$ GeV data. A sampling function of the form

$$f = p_{\perp}(a \exp(-p_{\perp}/w) + b/((1 + (r/\alpha)^{\beta})), \quad (9)$$

gives a satisfactory fit to the pp data in the Monte-Carlo.

Additionally, since we, for the moment, constrain our comparisons to the production of neutral pions in Au+Au we also present, in Figure (6), the PHENIX [48] mid-rapidity p_{\perp} yield for pp together with our representation of this spectrum.

The previous theoretical discussion [11, 12] strongly suggests that even moderately high p_{\perp} pre-hadrons, perhaps as low as 1 GeV/c, should be given hadron-like cross-sections. Furthermore, the earliest meson-meson collisions in our second phase cascade have an initial peak rate (in CM time) at $\sim .25-.35$ fm/c, with many collisions occurring at considerably later times. This permits even smaller pre-hadrons to appreciably increase their transverse size before colliding and simultaneously suggests that most collisions occur between co-moving pre-mesons.

D. Initial Conditions for Phase II

The final operation in phase I is to set the initial conditions for the cascade of pre-hadrons in phase II. Again we are guided in this by the elementary NN data mentioned above. The energy-momentum taken from the initial baryons and shared among the produced pre-hadrons is established and an upper limit is placed on the multiplicity of pre-hadrons. A final accounting of energy sharing is imposed through an overall 4-momentum conservation requirement.

The spatial positioning of the particles at this time could be accomplished in a variety of ways. For an AB collision we chose to place the pre-hadrons from each group inside a cylinder with transverse dimension determined by the group itself, given the initial longitudinal size of the interaction region at each impact parameter. We then allow the cylinder to evolve freely according to the longitudinal momentum distributions, for a fixed time τ_p , defined in the rest frame of each group. At the end of τ_p the total multiplicity of the pre-hadrons is limited so that, if given normal hadronic sizes appropriate to meson-meson cross-sections $\sim (2/3)(4\pi/3)(0.6)^3$ fm³, the pre-hadrons *do not overlap* within the cylinder. Such a limitation in density is consonant with the general notion that produced hadrons can only exist when separated from the interaction region in which they are generated [47]. One can conclude from this that the pre-hadron matter acts like an incompressible fluid, *viz.* a liquid, a state described in the earliest calculations with LUCIFER [6, 7].

Up to this point longitudinal boost invariance is completely preserved since phase I is carried out using straight line paths. The technique of defining the evolution time in the group rest frame is essential to minimizing residual frame dependence which inevitably arises in any cascade, hadronic or partonic, when transverse momentum is present. This dependence is due to the finite size of the colliding objects, implied by their non-zero interaction cross-section.

The collision history enumerates the number of interactions suffered by each baryon and allows us to assign baryon transverse momenta through random walk. Pre-hadron multiplicities, subject to the density restriction described above, are obtained using the KNO scaling we invoke for the elementary NN interactions and the known dependence on flavour. Production of baryon-antibaryon pairs is allowed, guided again by constraints from NN data. Transverse momentum is generated for the pre-hadrons and other produced particles, paying attention to the random walk increase for mesons created by multiple baryon-baryon collisions. Finally, overall energy-momentum conservation is imposed and with it the multi-particle phase space defined.

III. PHASE II: FINAL STATE CASCADE

We note that phase II is a relatively lower energy cascade with the collisions between pre-hadrons, for example, involving energies less than $s^{1/2} \sim 15$ GeV and even lower average energy. The sharing of energy-momentum in the original baryon groups with the produced mesonic pre-hadrons leads to appreciable energy loss from the initial baryons. This loss mirrors the initial gluon radiation energy losses described in the pQCD approach and as has been made clear occurs mostly before the characteristic time τ_p . Phase II is as stated a standard sequential cascade calculation in which the pre-hadrons interact and decay as do any normal hadrons either already present or produced during this cascade. This cascade of course imposes exact energy-momentum conservation at the level of two body collisions. For Au+Au, the effect of the pre-hadron interactions is truly appreciable, greatly increasing multiplicities and total transverse energy, E_\perp both through production and via eventual decay into the stable meson species, but also, as will be seen, leading to the suppression of high p_\perp hadron yields.

We are then in a position to present results for Au+Au collisions at 200 A-GeV. These appear in Figures (7–10) for various double differential transverse momenta spectra and their ratios. Most contain comparisons with PHENIX [4, 48] π^0 measurements. In future work we will consider also charged particle data, where produced proton spectra would play a larger role with increasing p_\perp . One expects however to see similar global behaviour for charged mesons.

IV. RESULTS: COMPARISON WITH π^0 DATA

Figures (5) and (6) show the input, nucleon-nucleon data for elementary production of π^0 's and charged particles. These transverse momentum spectra at mid-rapidity have been compared to results from PHENIX [48] and UA1 [43]. Figure (7) contains the simulated π^0 transverse momenta spectrum for Au+Au at $\eta = 0$ alongside the PHENIX data [4]. To a large extent the suppression observed experimentally is paralleled by the simulated calculations. The production time τ_p introduced above was given two values ($2R_{Au}/\langle\gamma\rangle$) and twice this value. The variation with this initial state time, a parameter in our modeling, was small. $\langle\gamma\rangle$'s here is the longitudinal Lorentz factor defined above and introduced for each baryon group separately in its rest frame.

It's evident from the figures that, most emphatically, one *cannot* ignore final state cascading. Moreover, with the assumptions we have made, the most crucial being perhaps the early commencement time for such cascading, the suppression cannot be considered as necessarily a sign for production of a quark-gluon plasma: the results may perhaps equally well signify only the creation of a pre-hadron dominated medium after a short initial delay $\sim \tau_p$. We repeat: despite the apparently short time τ_p at say $s^{1/2} = 200$ GeV, one finds in practice that the phase II collisions have an effective production or delay time of $0.25 - 0.35$ fm/c and continue for some tens of fm/c. 'Co-moving' collisions dominate the cascade.

It's instructive to dissect the contributions of the different phases of the simulation, *i.e.* to separately show the spectrum at the conclusion of phase I from that which results after both phases I and II are complete. In Figure (8) the π^0 transverse momentum yield is shown for both these cases against the experimental data. It is immediately evident that the many virtual NN collisions in phase I produce a much elevated p_\perp output and that this is in turn reduced by more than an order of magnitude by collisions with other pre-hadrons in phase II. Part of this effect is through inclusion in the dynamics of at least a kinematical treatment of energy loss. Thus the above analogy of an initial hot gas cooled by final state interactions during expansion, is apt.

One might well turn this around and declare that the final state scattering of a given pre-hadron with its co-movers has cut down the Cronin effect, a reduction which suggests the applicability of the term 'jet suppression' through final state interactions. One notes parenthetically that particles lost at high p_\perp are compensated for by an increase in those appearing at the lowest p_\perp 's. This is of course part of the effective cooling observed.

A second and equally important criterion for the simulation is the maximum density imposed on initial conditions for phase II. Figure (9) casts some light on this and on another issue, the actual transverse energy density attributed

to the earliest stages of the collision. We have included in this figure the charged $dN/d\eta$ spectra, including a BRAHMS charged meson result (compared to a simple fit):

- (a) for the totality of ‘stable’ mesons in phase I+II
- (b) the same result for phase I alone when only decays of pre-hadrons but no phase II re-interactions are permitted,
- (c) pre-hadrons in phase I with no decays

It is evident that some 2/3 of the summed transverse energy E_\perp is generated in the second expanding phase II when the system is increasing both longitudinally and transversely. The initial, very early, E_\perp generated is then reduced commensurately, falls well below the Bjorken limit and is hence not all available for initial coloured ‘plasma’ generation. In present calculations at the initialisation of II, and keeping in mind the average masses assigned to pre-hadrons centered at 0.8 to 1.0 GeV, the ambient transverse energy densities are $\leq 1.8 \text{ GeV}/fm^3$ for the shortest initial time τ_p chosen and correspondingly less for longer times. Lattice calculations [10], however, do consider such densities adequate for observation of the so-called cross-over transition.

A. Ratios of Au+Au to NN Production

In Figure (10) we display the often discussed ratio [2, 3, 5, 50] introduced in Eqn.(1). The discrepancies between simulation and data are magnified but the general agreement shown in Figure (3) remains intact. The direct double-differential cross-sections fall many orders of magnitude over the measured range of p_\perp but the ratios to normalized proton-proton data cover a much compressed range of p_\perp . In this figure we presented PHENIX π^0 data from an early paper [4], but more recent data [51] tells a somewhat modified tale. The dip in $R[\text{AuAu}/\text{NN}]$ at the lowest transverse momentum point $p_\perp = 1.25 \text{ GeV}/c$, implying a maximum in this ratio at slightly higher p_\perp , has apparently disappeared. This is so for both the 0 – 5% and 0 – 10% central data resulting in curves in better agreement with the corresponding theoretical calculations at the measured p/p_{pp} ’s. The equivalent charged particle ratios [2, 3, 5, 50] still exhibit the apparent maximum, but in a region where the proton spectra show considerable activity. One might also question the use of the ratio $R[\text{AA}/\text{NN}]$ at very low p_\perp , involving as it does the number of binary collisions. A relevant or preferred divisor there might be the number of participants.

The pQCD arguments given above for the early de-colourisation of the initial medium would only apply to sufficiently hard mesons, perhaps $p_\perp \sim 1 \text{ GeV}/c$ or greater. Nevertheless, our soft hadronic approach for the lower transverse momenta does apparently give a good description of the spectra at the lowest p_\perp ’s as well.

In Figure (10) we present LUCIFER calculations for 0% – 10% centrality, but the shape is generic at least for reasonably central collisions. As one approaches extreme peripherality the ratio will at all p_\perp eventually approach unity, provided of course the number of binary collisions N_{coll} is also adjusted.

It’s worth repeating that no additional adjustable parameters, beyond the times for production, τ_p , and hadronisation (decay of pre-hadrons), τ_f , were, nor would such an approach be consistent with our goals. We seek only a qualitative and reasonably quantitative understanding of the observations.

The simulations performed here overestimate, but not by very much, the suppression of the spectrum at the lowest p_\perp , but yield an overall, perhaps surprisingly, accurate description.

V. CONCLUSIONS

An alternative interpretation of the high transverse momentum suppression in Au+Au has been presented. We have employed a pQCD argument to justify the production of pre-hadrons at early times within our simulation, and the presence of relatively large objects leads to a great deal of scattering in the final state cascade. It’s this rescattering that produces the ‘jet’ suppression in our picture. Of course, and paradoxically, it is to the higher p_\perp mesons at RHIC that the pQCD argument best applies. It is, however, interesting to extend our treatment to the lower reaches of the spectrum for the ratio $R[\text{AuAu}/\text{NN}]$. Certainly there is still a silent elephant lurking in the background: the observation of rather large elliptical flow in the meson spectrum [16]. These flow measurements are most easily reproduced theoretically in parton cascade models when hadron-sized cross-sections are invoked [15], and cross-sections of this magnitude are what our pre-hadron cascade employs.

In the work on D+Au [1] the use of such a pre-hadron spectrum exposed most clearly the simple role of dynamically-driven geometry in ratios of BRAHMS p_\perp spectra at varying η , suppression in this case actually occurring only at high η .

For Au+Au the modification of the p_{\perp} spectra during phase II of LUCIFER is considerably increased and suppression is seen even at $\eta = 0$. Certainly, the RHIC experiments are creating unusual nuclear matter, at high hadronic and energy density, with exciting consequences. Surely more experimental exploration is required.

One important, if controversial, aspect of our combined pQCD justification of pre-hadrons together with their subsequent phase II cascade, is the likelihood that hadronic measurements are not necessarily probing the earliest coloured stages of the AA interaction. To illuminate this coloured phase it may be necessary to invoke dilepton or direct γ signals. In fact 10 GeV jets are, for the full RHIC energy $s^{1/2} = 200$ GeV, not perhaps the ‘purest’ jets in a pQCD approach, and one can perhaps reach even higher transverse momentum, $p_{\perp} > 10 - 12$ GeV/c, for signs of deviation from the so far observed suppression.

VI. ACKNOWLEDGEMENTS

This manuscript has been authored under the US DOE grant NO. DE-AC02-98CH10886. One of the authors (SHK) is also grateful to the Alexander von Humboldt Foundation, Bonn, Germany and the Max-Planck Institute for Nuclear Physics, Heidelberg for continued support and hospitality. Useful discussion with the BRAHMS, PHENIX, PHOBOS and STAR collaborations are gratefully acknowledged, especially with C. Chasman, R. Debbé, F. Videbaek, D. Morrison, M. T. Tannenbaum, T. Ulrich and J. Dunlop.

-
- [1] D. E. Kahana and S. H. Kahana, nucl-th/0406074; Phys. Rev. **C72**, 024903, (2005).
 - [2] I. Arsene *et al.*, BRAHMS Collaboration, Phys. Rev. Lett., **91** 072305, (2003); R. Debbé, BRAHMS Collaboration nucl-ex/0403052; I. Arsene *et al.*, the BRAHMS, nucl-ex/0307003; I. Arsene *et al.*, the BRAHMS Collaboration, nucl-ex/0403050; I. Arsene *et al.*, nucl-ex/0307003.
 - [3] B. B. Back *et al.*, PHOBOS Collaboration, Phys. Lett., **461**, 297, (2004); B. B. Back *et al.*; B. B. Back *et al.*, the PHOBOS Collaboration, Phys. Rev. Lett., **91** 072302-1, (2003).
 - [4] S. S. Adler *et al.*, PHENIX Collaboration, Phys. Rev. C. **69**, 034910, (2004); Phys. Rev. Lett. **91**, 072301, 2003; K. Adcox *et al.*, nucl-ex/0207009.
 - [5] C. Adler *et al.*, STAR Collaboration, Phys. Rev. Lett. **91**, 172302, 2003; Phys. Rev. Lett. **89**, 202301, (2002); J. Adams *et al.*, Phys. Rev. Lett. **91** 172302, 2005.
 - [6] D. E. Kahana and S. H. Kahana, *Proceedings, RHIC Summer Study’96*, 175-192, BNL, July 8-19, 1996; D. E. Kahana and S. H. Kahana, Phys. Rev. **C58**, 3574 (1998); Phys. Rev. **C59**, 1651 (1999).
 - [7] D. E. Kahana, S. H. Kahana, Phys. Rev. **C63**, 031901 (2001).
 - [8] Proc. International Conference on the Physics of the Quark-Gluon Plasma, Ecole Polytechnique, Palaiseau, France, Sept. 4-7, 2001; D. E. Kahana, S. H. Kahana, nucl-th/0208063.
 - [9] E. V. Shuryak and I. Zahed, hep-ph/0307267; and hep-th/0308073.
 - [10] S. Datta, F. Karsch, P. Petreczky and I. Wetzorke, hep-lat/0208012; hep-lat/0403017; hep-lat/0309012.
 - [11] B. Z. Kopeliovich, J. Nemchik, I. Schmidt, Nucl. Phys. A **782** 224-233, 2007.
 - [12] E. Berger. Z. Phys **C4** 289, 1984.
 - [13] F. Niedermayer, Phys. Rev. **D34** 3494, 1986.
 - [14] R. J. Glauber, in *Lectures in Theoretical Physics*, edited by W. E. Brittin *et al.*, Interscience, New York, 1959, Vol. I, p.315.
 - [15] D. Molnar and M. Gyulassy, nucl-th/0102031; nucl-th/0104018; D. Molnar, presentation at workshop on “Creation and Flow of Baryons in Hadronic and Nuclear Collisions”, ECT, Trento, Italy, May 3-7, 2004 (unpublished).
 - [16] S. S. Adler *et al.*, the PHENIX Collaboration, Phys. Rev. Lett. **91**, 182301 (2003); C. Adler *et al.*, the STAR Collaboration, Phys. Rev. Lett. **87**, 182301 (2001), S. Manly, the PHOBOS Collaboration, Proceedings of the 20th Winter workshop on Nuclear Dynamics, Trelawney Beach, Jamaica, March 15-20, 2003.
 - [17] H. Stoecker and W. Greiner, Phys. Rep. **137**, 277 (1986); R. Mantiello, A. Jahns, H. Sorge and W. Greiner, Phys. Rev. Lett., **74**, 2180 (1995).
 - [18] H. Sorge, Phys. Rev. **C52**, 3291 (1995).
 - [19] S. A. Bass *et al.*, Nucl. Phys. A **661**, 205 (1999).
 - [20] B. Andersson, G. Gustafson, G. Ingelman, and T. Sjostrand, Phys. Rep **97**, 31 (1983); B. Andersson, G. Gustafson, and B. Nilsson-Almqvist, Nucl. Phys B **281**, 289 (1987).
 - [21] A. Capella and J. Tran Van, Phys. Lett. **B93**, 146 (1980) and Nucl. Phys. A **461**, 501c (1987); A. Capella *et al.*, nucl-th/0405067 and hep-ph/0403081.
 - [22] K. Werner, Z. Phys. **C42**, 85 (1989); K. Werner, J. Aichelin, Phys. Rev. Lett. **76** (1996) 1027-1030; H. J. Drescher, M. Hladik, S. Ostapchenko, K. Werner, Proc. of the “Workshop on Nuclear Matter in Different Phases and Transitions”, Les Houches, France, March 31 - April 10, 1998; K. Werner Invited lecture, given at the Pan-American Advanced Study Institute “New States of Matter in Hadronic Interactions” Campos de Jordao, Brazil, January 7-18, 2002, hep-ph/0206111.
 - [23] B. Zhang, C. M. Ko, B.-A. Li, Z. Lin, nucl-th/9904075; Z. Lin and C. M. Ko, Phys. Rev. C **68**, 054904 (2003); Z. Lin *et al.* Nucl. Phys. A **698**, 375-378 (2002).

- [24] J. Ranft and S. Ritter, Z. Phys. C**27**, 413 (1985); J. Ranft Nucl. Phys.A**498**, 111c (1989).
- [25] D. Boal, *Proceedings of the RHIC Workshop I*, (1985) and Phys. Rev. C**33**, 2206 (1986).
- [26] K. J. Eskola, K. Kajantie and J. Lindfors, Nucl. Phys. B**323**, 37 (1989).
- [27] X. -N. Wang and M. Gyulassy, Phys. Rev. D**44**, 3501 (1991); X. -N. Wang, nucl-th/000814 and nucl-th/0405029; X. -N. Wang hep-ph/0405125.
- [28] M. Gyulassy and X. N. Wang, Comp. Phys. Comm. **83**, 307 (1994),
- [29] K. Geiger and B. Mueller Nucl. Phys. B**369**, 600 (1992); K. Geiger Phys. Rev. D**46**, 4965 and 4986 (1992); K. Geiger, *Proceedings of Quark Matter'83*, Nucl. Phys. A **418**, 257c (1984); K. Geiger, Phys. Rev. D **51**, 2345 (1995).
- [30] S. A. Bass, B. Mueller and D. K. Srivastava, Phys. Rev. Lett.B **551**,277 (2003); S. A. Bass *et al.*, Nucl. Phys. A**661**, 205 (1999).
- [31] K. Gallmeister, C. Greiner and Z. Xu, Phys. Rev. C**67**, 044905 (2003).
- [32] W. Cassing, K. Gallmeister, C. Greiner Nucl.Phys. A735, 277-299 (20004); J. Geiss, C. Greiner, E. Bratkovskaya, and U. Mosel, Phys. Lett. B**447**, 31 (1999).
- [33] G. Wolschin, Europhy. Lett **74**, (2006), 29-35; Annalen Phys. **15**,(2006), 369-378; Phys. Rev. **69**,(2004), 024906.
- [34] L. V.Gribov, E. M.Levin and M. G. Ryskin, Phys. Rep. **100**, 1 (1983); Nucl. Phys. B**188**, 555 (1981); A. H. Mueller and J. Qiu, Nucl. Phys. B**268**,427 (1986); E. M.Levin and M. G. Ryskin, Phys. Rep. **189**, 267 (1990).
- [35] L. McLerran and R. Venugopalan, Phys. Rev. D**49**, 2223 (1994); Phys. Rev. D**59**, 094002 (1999); D. Kharzeev, E. Levin and L. McLerran, Phys. Lett. B**561**, 93 (2003).
- [36] D. Kharzeev, E. M.Levin and L. McLerran hep-ph/0210332 (2002); L. McLerran hep-ph/0402137 (2004); D. Kharzeev, E. M.Levin and L. McLerran, hep-ph/0403271 (2004).
- [37] K. Goulianos, *Phys. Rep.***101**, 169 (1983).
K. Goulianos, *Phys. Rep.***101**, 169 (1983).
- [38] V. Ezhela, S. Lugovsky, N.Tkachenko, and Yu. Kuyanov. IHEP, Protvino, Russia, August 2005, in The review of particle Physics, W-M Yao et al. Phys.G33(2006).
- [39] Giorgio Chiarelli for the CDF Collaboration, *Proceedings of the Topical Workshop on Proton-Antiproton Collider Physics* October 18-22, 1993. Tsukuba, Japan; F. Abe *et al.* Phys. Rev. D**50**,550-5561,1994.
- [40] Z. Koba,H. B. Nielsen, and P. Olesen,Nucl. Phys., B40 317, 1972.
- [41] UA5 Collaboration, Phys. Lett. B**561**, 93 (2003).
- [42] G. Ekspog for the UA5 Collaboration, Nucl. Phys.A**461**, 145c (1987); G. J. Alner for the UA5 Collaboration, Nucl. Phys.B**291**, 445 (1987).
- [43] C. Albajar *et al.*, the UA1 Collaboration, Nucl. Phys. B**335**, 261-287 (1990).
- [44] Y. Eisenberg *et al.*, Nucl. Phys. A**461**, 145c (1987) G. J. Alner *et al.*, Nucl. Phys. B **291**, 445 (1987); F. Abe et al., Phys. Rev.**D41** 2330, (1990).
- [45] B. B. Back *et al.*, the PHOBOS Collaboration, Phys. Rev. Lett. **88**, 22302 (2002).
- [46] J. W.Cronin *et al.*, Phys. Rev. D**91**, 3105 (1979).
- [47] K. Gottfried, Phys. Rev. Lett. **32**, 957 (1974); and Acta. Phys. Pol B**3**, 769 (1972).
- [48] S. S. Adler *et al*, PHENIX Collaboration, Phys. Rev. Lett. **91** 241803, (2003).
- [49] I. L. Arsene *et al*, BRAHMS Collaboration, nuc-ex/0403050,(2004).
- [50] K. Adcock *et al*, PHENIX Collaboration, nucl-ex/0207009.
- [51] M. Shimamura, for the PHENIX Collaboration, nucl-ex/0510023.

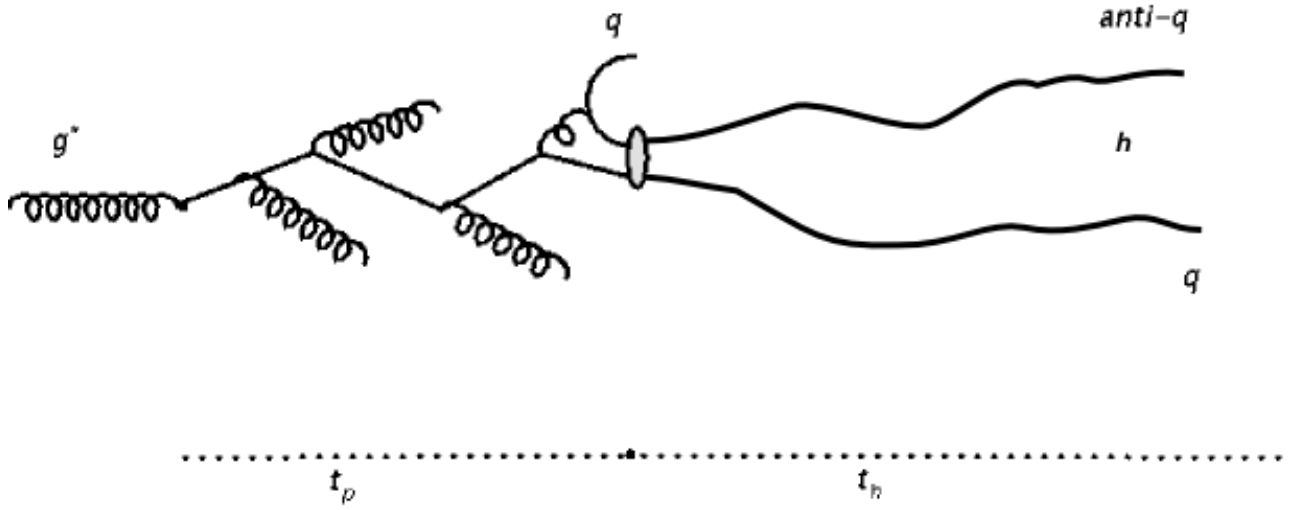


FIG. 1: Schematic drawing, borrowed from Kopeliovich et. al [11], of the perturbative formation of a pre-hadron from an off-shell gluon g^* incident on a quark in the rest frame of nucleus B in an A+B or P+B event. The quark radiates gluons and eventually combines with a perturbatively produced anti-quark to form at first a small colourless pre-hadron which rapidly expands to hadronic size. The time t_p signifies the production time of the pre-hadron and t_h its later hadronisation time. It is argued in the text that in general t_p is much less than t_h , and the existence of two such time scales is critical to the parton-hadron dynamics.

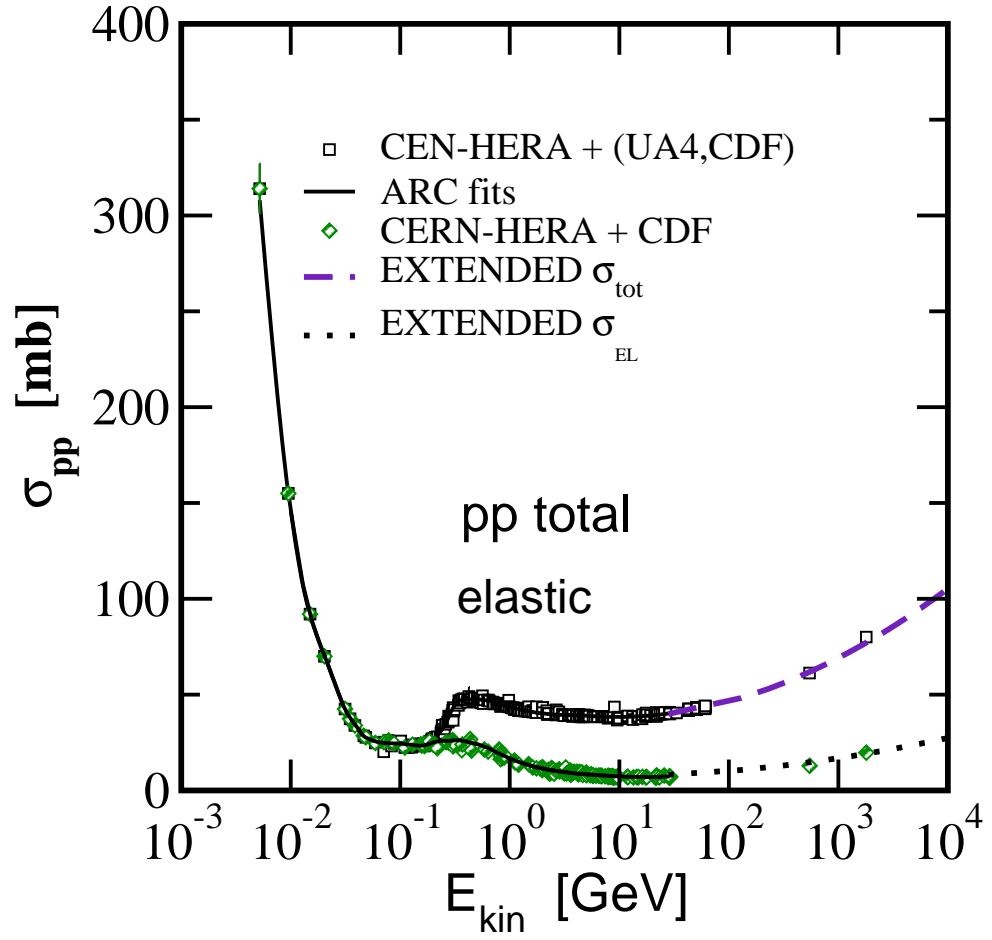


FIG. 2: Total and Elastic cross-sections: Comparison of data compilations from a variety of sources, CERN-HERA, UA1,4,5 and CDF, with the fits used in LUCIFER.

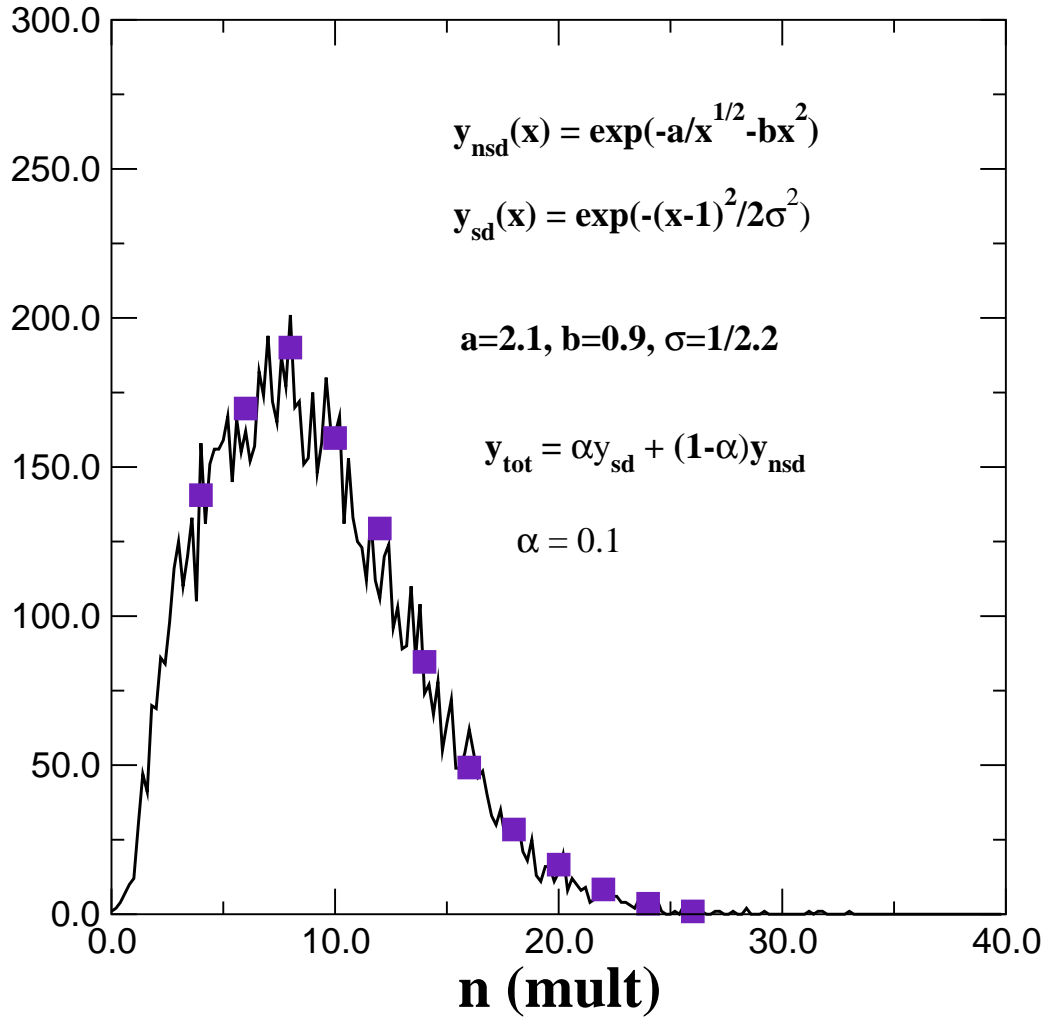


FIG. 3: Multiplicity Distributions: Data for $s^{1/2} = 26$ GeV is compared to a histogram using the KNO scaling outlined on this figure. The histogram is obtained from a reasonable number of pp events, and of course is itself normalized to a probability distribution. Clearly the same KNO distribution is used at all energies with $x = n/\bar{n}$.

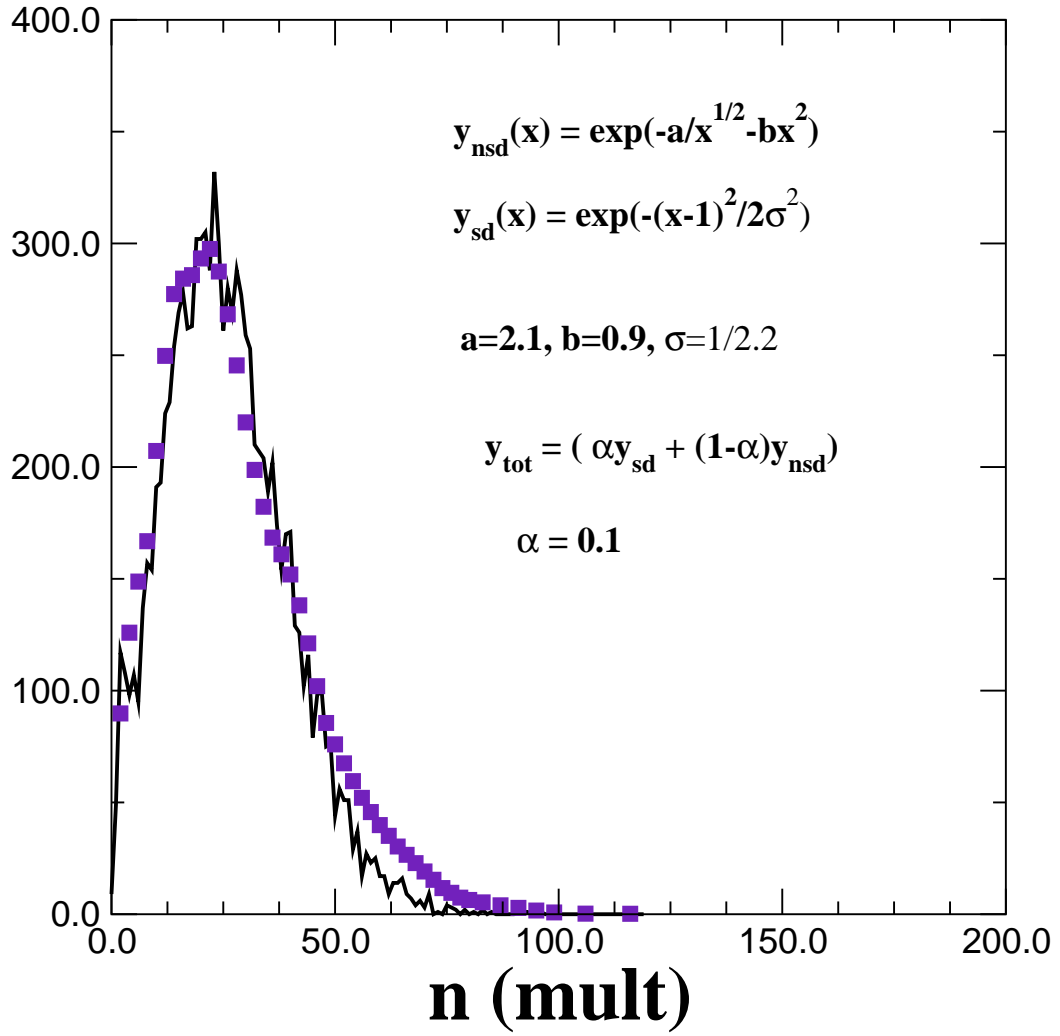


FIG. 4: Multiplicity Distributions: Data for $s^{1/2} = 546$ GeV is compared to a histogram using the KNO scaling outlined on this figure. The strict KNO scaling seems to fail in the high multiplicity tail of the distribution shown here, but in a fashion which very little influences our A+A simulations. Clearly the same KNO distribution is used at all energies.

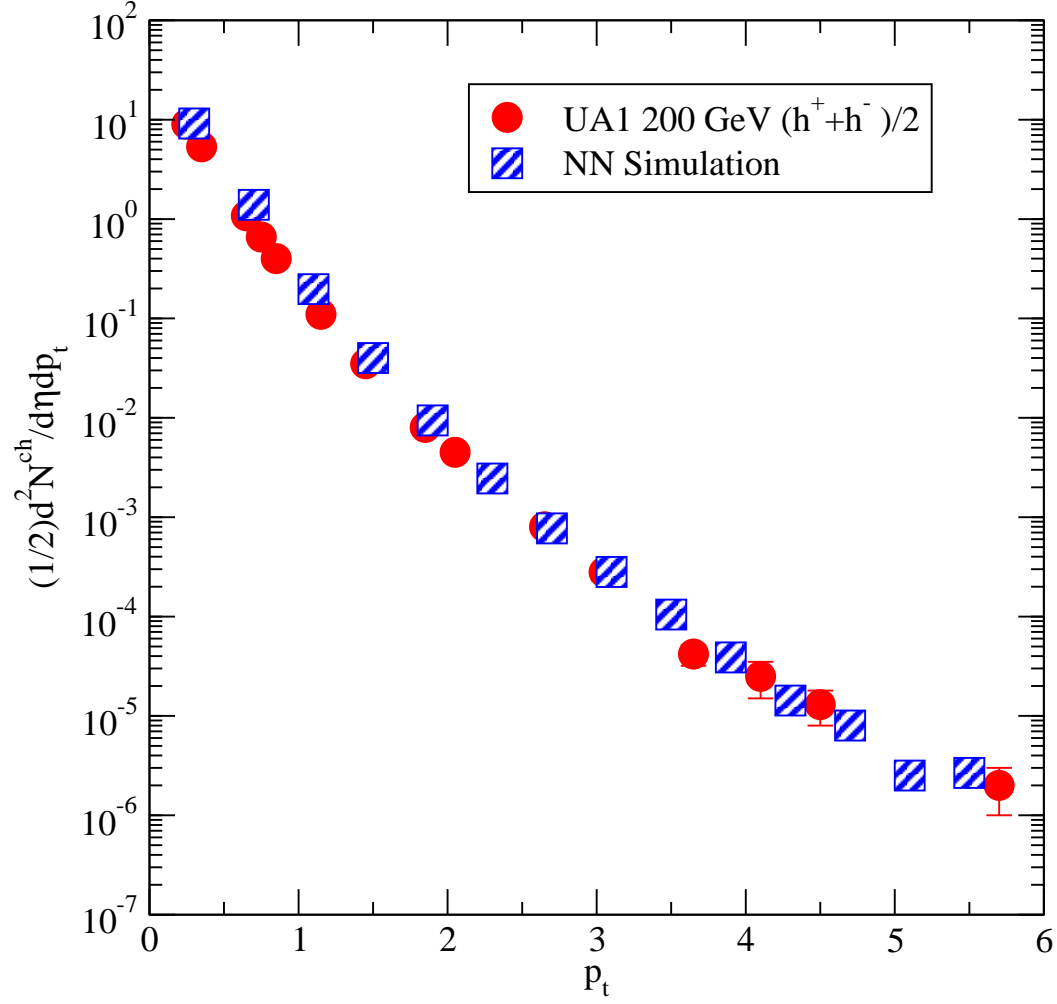


FIG. 5: pp Pseudo-rapidity spectra: Comparison of UA1 minimum bias 200 GeV NSD data [43] with an appropriate LUCIFER simulation. The latter is properly constrained by experiment and is an input to the ensuing AA collisions; thus does not constitute a ‘set’ of free parameters.

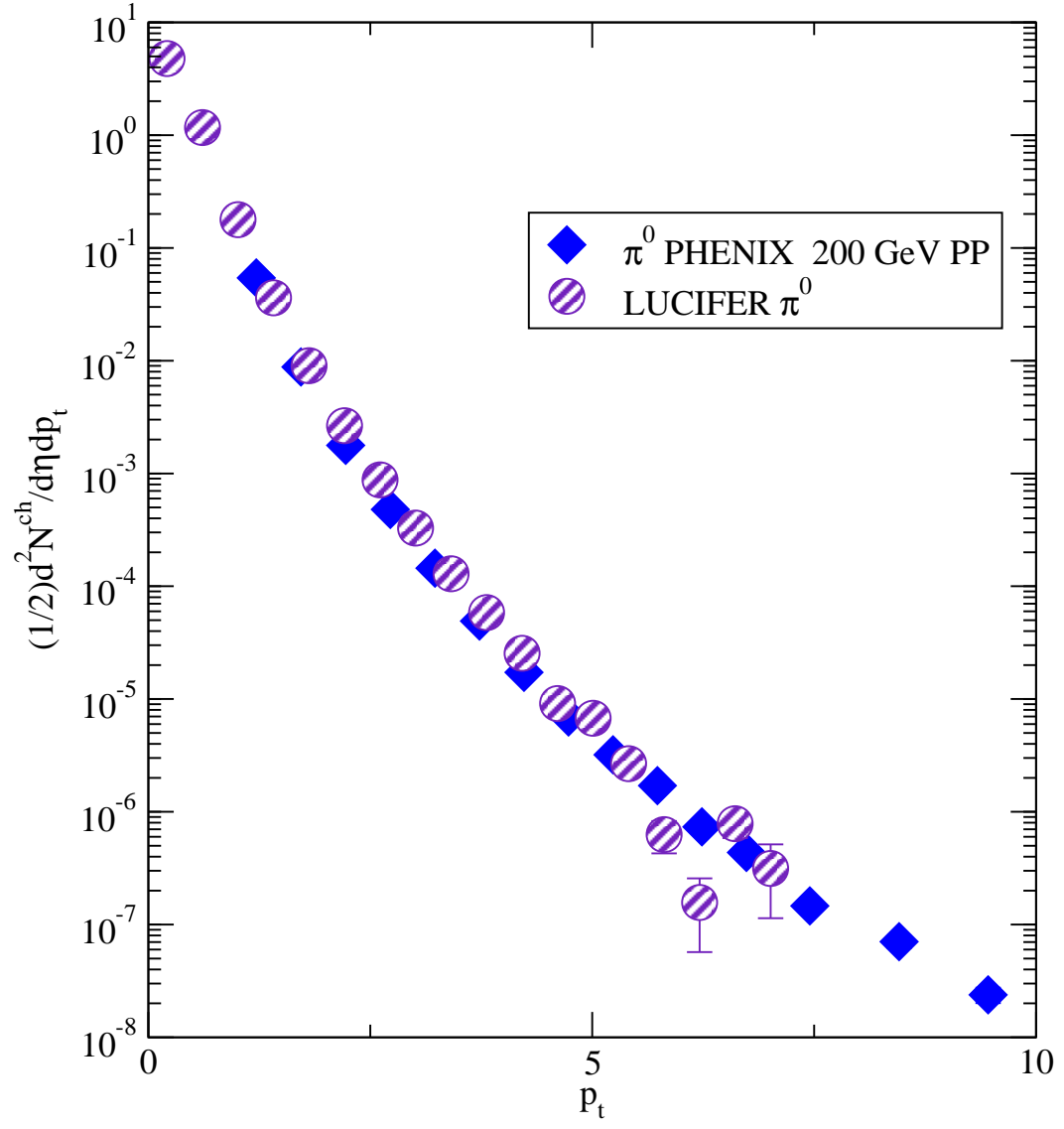


FIG. 6: A similar transverse momentum π^0 spectrum from PHENIX pp [48] vs simulation.

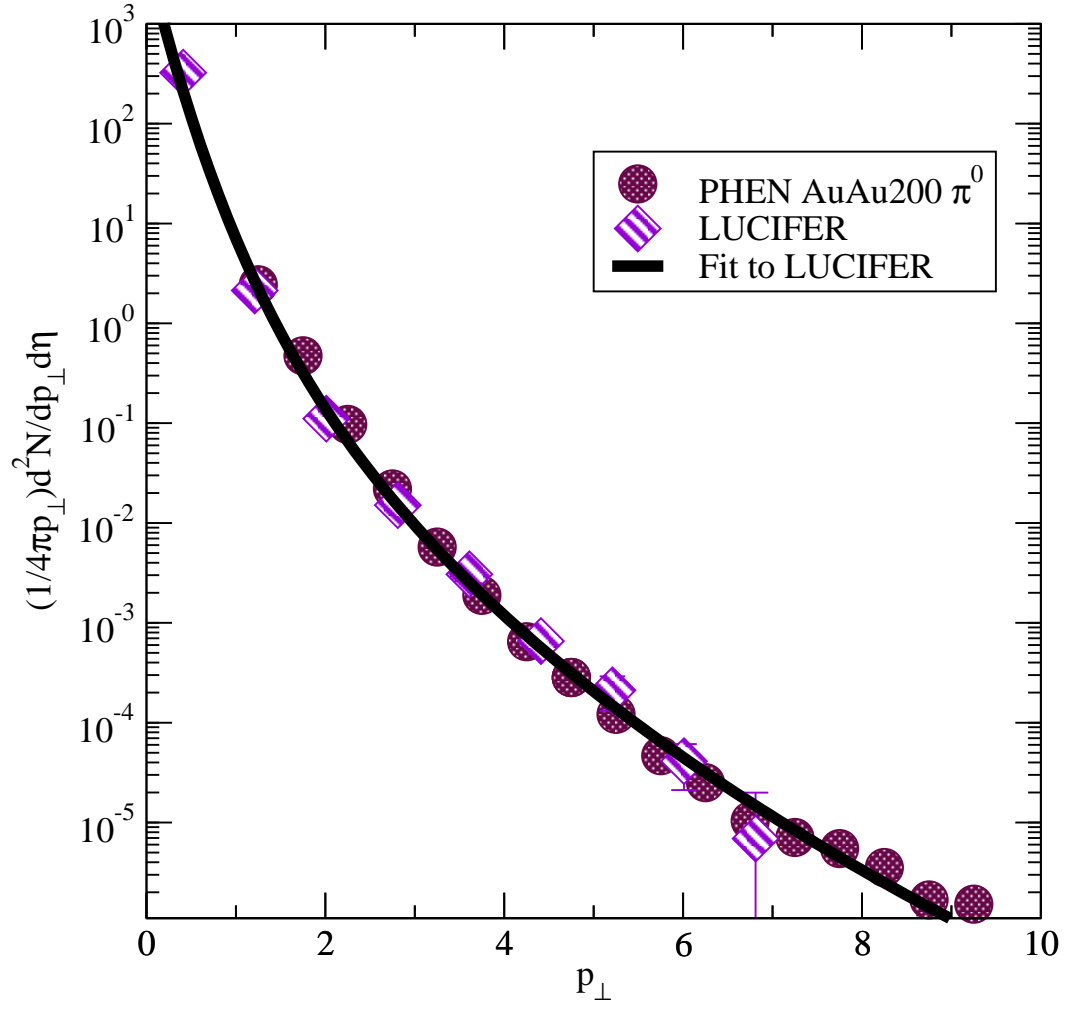


FIG. 7: Central PHENIX π^0 200 GeV for Au+Au vs simulation. Curves for different choices of the production time τ_p differ very little, since in effect the cascade effectively begins somewhat later, near $0.25 - 0.35$ fm/c and continues much longer to tens of fm/c. Centrality for PHENIX is here 0% – 10%, roughly for impact parameters $b < 4.25$ fm. in the simulation.

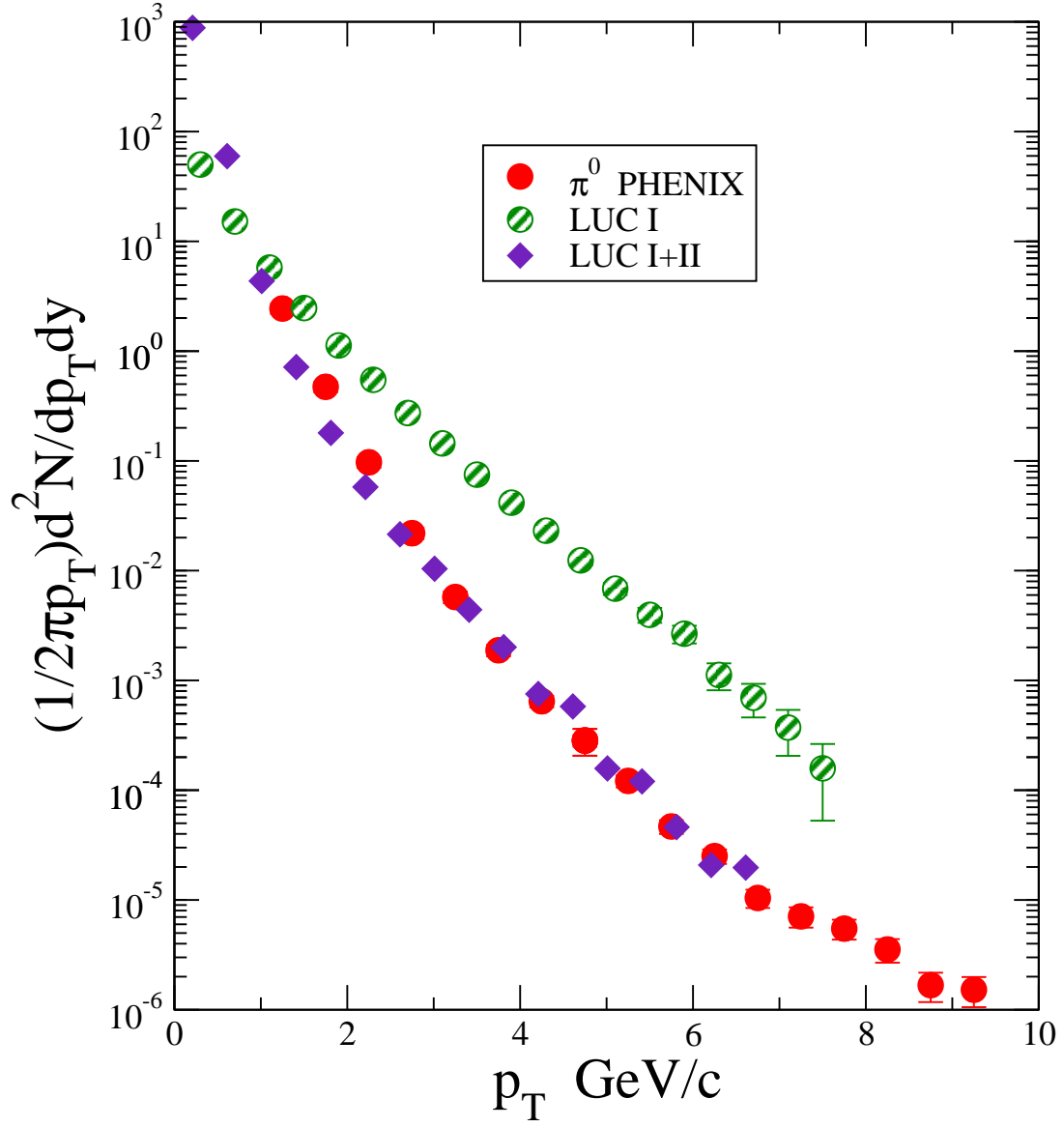


FIG. 8: The π^0 transverse momenta yields for phase I, no final cascade, vs those for the full phase I+II calculation. Clearly there is considerable suppression in the final cascade. Recalling that the experimentalists quote a ‘direct’ suppression of ~ 4 – 5 for the ratio in Eqn.(1) at the highest p_\perp , there is at the end of I an enhancement ~ 3 , *i. e.* still a Cronin effect in this first phase.

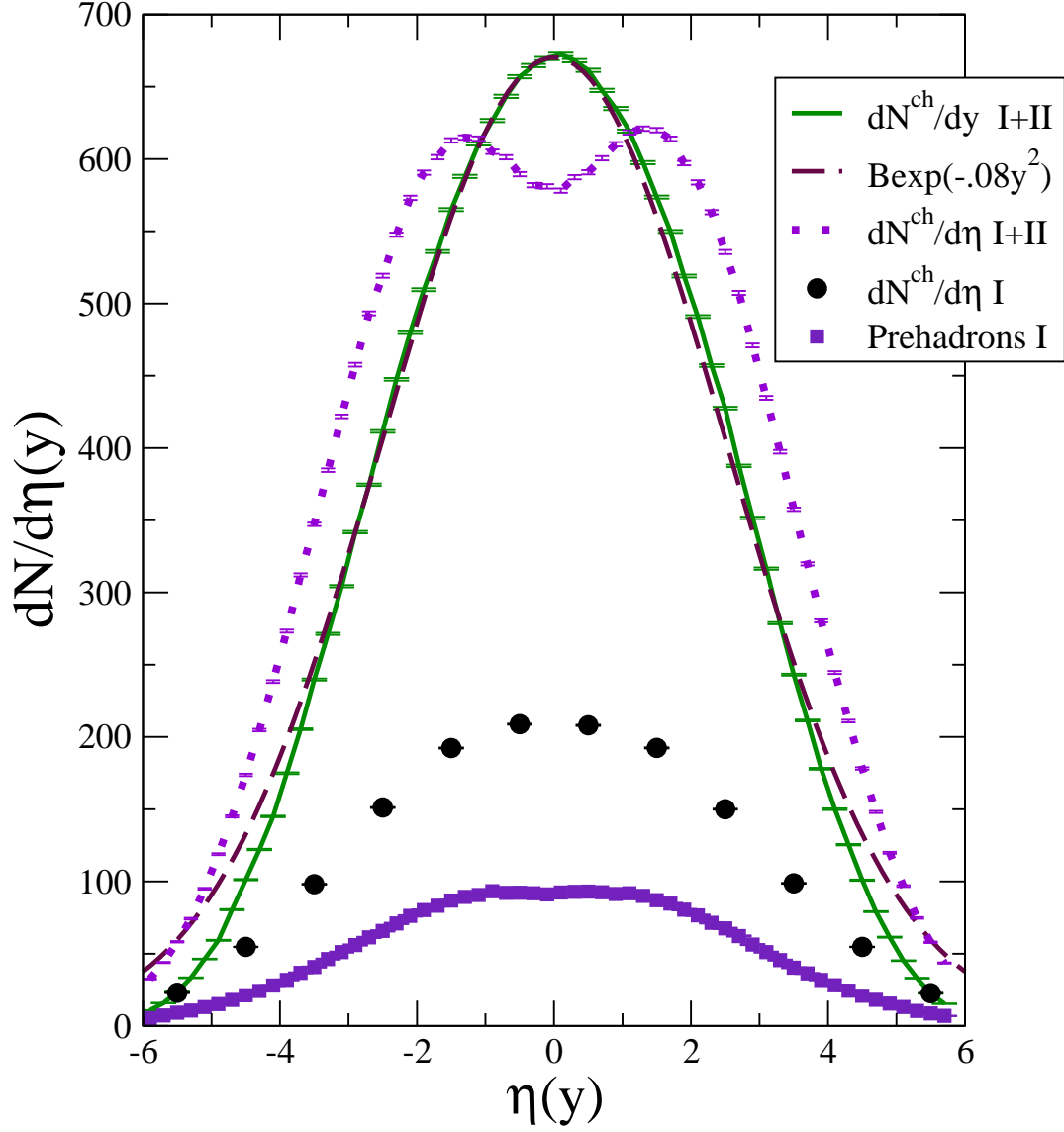


FIG. 9: Pseudo-Rapidity and rapidity spectra for charged mesons and pre-hadrons at various phases of the collision simulation. The Gaussian fit (dashed line) to the charged pion rapidity distribution approximates preliminary BRAHMS dN^{ch}/dy [49] results, certainly in its FWHM, and hence demonstrates the validity of the simulation (solid line) for dN^{ch}/dy . A calculation for $dN^{ch}/d\eta$ (dotted line) is also presented. For the charged pseudo-rapidity distributions, successive retreats, first to phase I of the simulation (solid circles) and then to only pre-hadrons in phase I (solid rectangles), *i. e.* no decays, indicates both the reduction in cascading participants and in the fraction of E_{\perp} available at the earliest moments of the cascade.

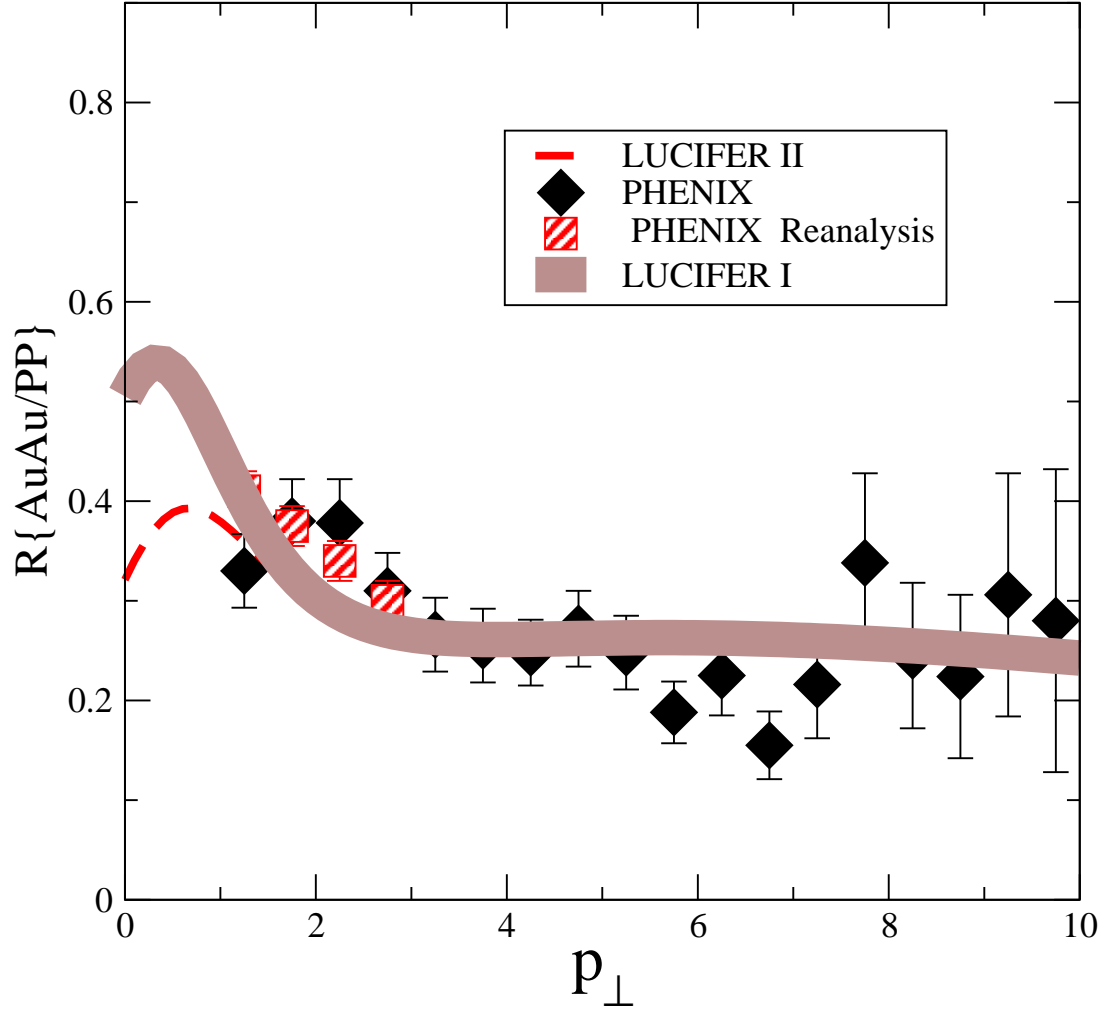


FIG. 10: $R_{AuAu/NN}$: Ratio of π^0 production in $Au + Au$ collisions to that in NN at $s^{1/2} = 200$ GeV for 0%–10% centrality. The binary collision number selected at this centrality is $N_{coll}=950$, while the divisor for both PHENIX and LUCIFER curves shown here are ones fit to the PHENIX pp data. The resultant ratio is especially sensitive to the PHENIX NN data. LUCIFER curves are shown for two choices A and B differing not in the $Au + Au$ calculations but only in the fitted PHENIX NN extrapolation to lowest p_{\perp} , where of course there is no data. The extra points for the PHENIX AuAu ratio at the four lowest p_{\perp} GeV/c are from more recent analysis [51]. Thus the general shape and magnitude of the simulation conforms well with this most recent data analysis, both exhibiting a rise toward smaller p_{\perp} . This feature is also present in the very similar 0% – 5% measurement [51]. The calculated suppression is somewhat excessive at low p_{\perp} .

